Available online at www.sciencedirect.com

SciVerse ScienceDirect

Ceramics International 39 (2013) 7273–7277

CERAMICS INTERNATIONAL

www.elsevier.com/locate/ceramint

Short communication

Synthesis, microstructure and mechanical properties of reactively sintered ZrB_2–SiC–ZrN composites

Wen-Wen Wu[a,*], Guo-Jun Zhang[b], Yan-Mei Kan[b], Yoshio Sakka[a,*]

[a]*Advanced Ceramics Group, National Institute for Materials Science (NIMS), Tsukuba, Ibaraki 305-0047, Japan*
[b]*State Key Laboratory of High Performance Ceramics and Superfine Microstructures, Shanghai Institute of Ceramics, Shanghai 200050, China*

Received 4 January 2013; received in revised form 16 January 2013; accepted 12 February 2013
Available online 19 February 2013

Abstract

ZrB_2–SiC–ZrN composites were fabricated by reactive hot pressing using Zr, Si_3N_4, and B_4C powders as starting materials. Sintering was conducted at temperatures of 1800 to 2000 °C under a load of 20 MPa in Ar atmosphere. The composite was densified at 2000 °C. The *in situ* formed BN flakes which distributed uniformly at the grain boundaries were identified by X-ray diffraction and scanning electron microscopy. The formation of *h*-BN phase and its effect on the mechanical properties of the composite are discussed.
© 2013 Elsevier Ltd and Techna Group S.r.l. All rights reserved.

Keywords: C. Mechanical properties; Microstructure; BN; Reactive hot pressing; ZrB_2

1. Introduction

Transition metal borides, ZrB_2 and HfB_2, which are known as ultra-high melting temperature ceramics (UHTCs), are attractive for applications that require exposure to extreme thermal and chemical environments such as those associated with atmospheric re-entry, hypersonic flight, and rocket propulsion [1]. Composites of diborides combined with silicon carbide (ZrB_2–SiC, HfB_2–SiC) have received great attention in the last decade, for their enhanced oxidation resistance in the temperature range of ~1100–1600 °C [2–4]. Because of their strong covalent bonding and low diffusion rates that inhibit the material transport required for densification, high sintering temperatures and hot pressing of the mixed powders are needed to achieve dense ceramics with desirable microstructure. Besides, various sintering aids, such as transition metal silicides ($MoSi_2$, $ZrSi_2$, and $TaSi_2$) [5–9], carbon and carbides (WC, ZrC, and B_4C) [10–14], and nitrides (Si_3N_4, AlN, HfN, and ZrN) [15–18] have been added into ZrB_2 to enhance its sinterability by forming a liquid phase or reacting with the oxides layer on the surfaces of the starting ZrB_2 particles.

In an attempt to create materials with moderate sintering temperatures, controlled novel microstructures, and high chemical compatibility of *in situ* formed individual phases, reactive sintering can play a significant role in further development of UHTCs processing. The highly exothermic elementary reactions between Zr metals and B and C, as well as the dissociative-replacement reaction between Zr and B_4C mixed powders, have been found effective for UHTC composite processing, provided that the exothermic reactions are well controlled. For example, high strength ZrB_2–SiC [19,20] and ZrB_2–SiC–ZrC [21,22] composites were prepared by reactive hot pressing (RHP) at mild temperatures of 1600–1800 °C. ZrB_2–$MoSi_2$ and ZrB_2–SiC–$MoSi_2$ composites [23] toughened with *in situ* synthesized elongated ZrB_2 grains were prepared by reactive hot pressing using Zr, Si, B/B_4C, and Mo as raw materials. ZrB_2–ZrN_{1-x} composites were *in situ* synthesized from Zr and *h*-BN powders by hot-pressing at 1800 °C [24].

In addition to silicides and carbides, which are commonly used as a secondary phase, the high melting point, high hardness, as well as its high thermal conductivity of ZrN suggest that it may also be a potential candidate for reinforcing phases. In the current work, a reaction was set to provide ZrB_2, SiC, and ZrN at the end of the process. Dense ZrB_2–SiC–ZrN composite was prepared by reactive hot pressing, using Zr, Si_3N_4 and B_4C powders as starting

*Corresponding authors. Tel.: +81 298592461; fax: +81 298592401.
E-mail addresses: WU.Wenwen@nims.go.jp (W.-W. Wu), SAKKA.Yoshio@nims.go.jp (Y. Sakka).

0272-8842/$ - see front matter © 2013 Elsevier Ltd and Techna Group S.r.l. All rights reserved.
http://dx.doi.org/10.1016/j.ceramint.2013.02.028

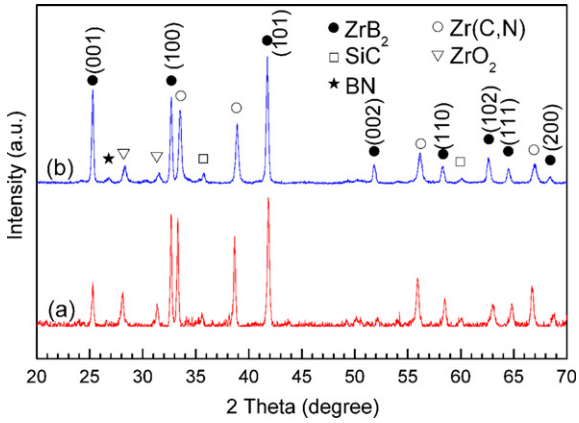

Fig. 1. XRD pattern of Zr–Si_3N_4–B_4C reactive hot pressed at: (a) 1800 °C/1 h and (b) 2000 °C/1 h.

materials according to the following reaction:

$$10Zr + Si_3N_4 + 3B_4C = 6ZrB_2 + 3SiC + 4ZrN \quad (1)$$

The reaction is thermodynamically favorable and exothermic, with a calculated reaction enthalpy of −2712.8 kJ/mol at 298 K, by using data from the NIST-JANAF tables [25]. The calculated volumetric composition (vol%) is $53.93ZrB_2 + 18.18SiC + 27.89ZrN$. The manufacturing process, microstructure, and the mechanical properties of the composites will be reported.

2. Experimental procedure

The correspondent stoichiometric precursors were weighed according to reaction (1). The starting powders were Zr, (purity > 98%, particle size < 28 μm, Beijing Mountain Technical Development Center for Non-ferrous Metals, Beijing, China), α-Si_3N_4 (UBE E-10, Ube Industries, Tokyo, Japan) and B_4C (purity ~99%, particle size about 2 μm, Jingangzuan Boron Carbide Co., Ltd, Mudanjiang, China). The powders were planetary ball milled in acetone at 550 rpm for 8 h in a polyethylene jar, using ZrO_2 balls as milling media. The weight ratio of the balls to powder was 2:1 and the diameter of the ball was 5 mm. The milled mixture was dried in a rotary evaporator to prevent powder segregation, sieved through a 200-mesh screen to reduce powder agglomeration, and then loaded in a graphite die with a BN coating. The mixture was reactive hot pressed in a resistance-heated graphite element furnace (ZT-60-22Y, Chen Hua Electric Furnace Co. Ltd., Shanghai, China) in an Ar atmosphere at a slow heating rate of 10 °C/min. The application of pressure (20 MPa) was loaded at 1550 °C. After the hot press was held at 1550 °C for 0.5 h, it was heated at 10 °C/min to target temperature and held for 1 h.

The bulk densities of the reactive hot pressed billets were determined using the Archimedes' method with distilled water as the immersing medium. Phase composition was conducted on the sample surface which is vertical to the hot pressing direction via X-ray diffractometry (XRD; D/Max-2250 V, Rigaku, Tokyo, Japan) using CuKa radiation. The microstructure analyses of the samples were conducted by an electron probe micro-analyzer (JXA-8100F, Tokyo, Japan) and by scanning electron microscopy (SEM; Hitachi S-570, Tokyo, Japan).

Three-point bending strength was measured on chamfered bars with dimensions of 3 mm × 4 mm × 36 mm using a span of 30 mm and a crosshead speed of 0.5 mm/min. Vickers hardness (Hv) and fracture toughness were tested by the indentation technique on polished samples (Wilson-wolpert Tukon @ 2100B, Instron, Boston, MA). Indentations were made using a 10 kg load with a dwell of 10 s. The fracture toughness was calculated based on the equation used in previous work [18]. Young's modulus was obtained from the slope of the flexural curve at the initial linear domain. Each data was an average of five measurements.

3. Results and discussion

3.1. Reactive sintering of ZrB_2–SiC–ZrN composites

Fig. 1(a) and (b) shows the XRD patterns of Zr, Si_3N_4 and B_4C mixtures that were reactive hot pressed at 1800 °C and 2000 °C, respectively. In both conditions, the main phases that formed were ZrB_2, ZrN, β-SiC, and no residual Zr was observed, which is consistent with reaction (1). The presence of ZrO_2 can be attributed to oxide impurities on the surface of starting powders or introduction of ZrO_2 media during planetary milling. Additional peaks of *h*-BN were also detected after the sintering temperature increased to 2000 °C. With the reactive hot pressing temperature increasing from 1800 °C to 2000 °C, the ZrN peaks shifted to a higher angle. Lattice parameters were calculated according to the XRD data in Fig. 1 using Jade 5.0 software. The calculated lattice parameter of this ZrN phase is 4.6277 Å with the estimated standard deviation of least-squares fits (ESD) of 0.00052, right between that of ZrC and ZrN, which is 4.6930 Å and 4.5776 Å, respectively. This calculated value is near to that of Zr_2CN, for which the lattice parameter is 4.625 Å.

According to reaction (1), the calculated theoretical density (g/cm^3) of the obtained composite is 5.90, based on the rule of mixtures and the densities of 6.09, 3.21 and 7.32 for ZrB_2, SiC and ZrN, respectively. However, the real densities measured by Archimedes' method were much lower than the theoretical one, with a maximum relative density of 90.2% after sintered at 2000 °C (shown in Table 1). On the other hand, with the increasing of sintering temperature from 1800 °C to 2000 °C, the open porosity decreased from 1.1% to 0.3%. No obvious closed pore can be seen in the microstructure of the sample that sintered at 2000 °C (shown in Fig. 3).

The chemical reactions of ZrB_2, SiC and ZrN were investigated in order to better understand the phase evolution under high temperature. A commercial software of HSC Chemistry version 6.1 [26] was used to calculate the equilibrium composition based on the Gibbs energy minimization method. For the calculation, the start

Table 1
Sintered density and open porosity of ZrB_2–SiC–ZrN composites after reactive hot pressing at different temperatures.

Sintering temperature (°C)	Density (g/cm^3)	Relative density (%)	Open porosity (%)
1800	5.11	86.6	3.5
1900	5.29	89.7	1.1
2000	5.32	90.2	0.3

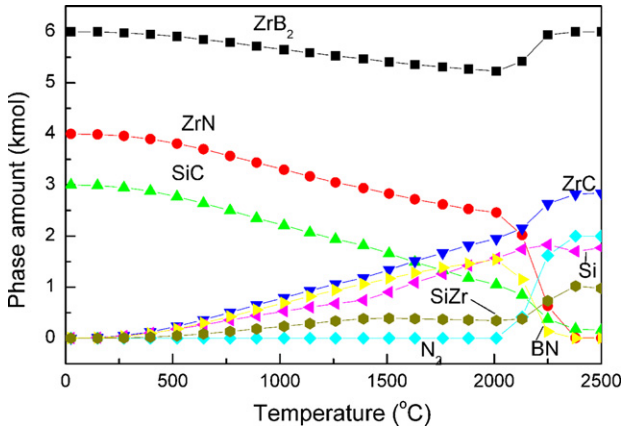

Fig. 2. Equilibrium composition as a function of the temperature, calculated at 1 bar Ar atmosphere.

composition was set as $6ZrB_2$ (s)+3SiC (s)+4ZrN (s), which is the product composition of reaction (1). All the species of the system were chosen for the calculation, including ZrC (s), N_2 (g), BN (s), C (s), B_4C (s), Si_3N_4 (s), Zr (s), Si (s), ZrSi (s), Zr_3Si_2 (s), Zr_5Si_3 (s), and $ZrSi_2$ (s). The equilibrium pressure was set to 1 bar of Ar atmosphere and the temperature range was set from 25 °C to 2500 °C. Fig. 2 shows the equilibrium composition of the prevailing phases during the reaction as a function of the temperature. Below 2000 °C, the amount of ZrB_2, SiC and ZrN show a steady decrease as temperature increased, meanwhile, the amount of ZrC, Si, SiZr and BN increased. It was assumed ZrN decomposes at low temperature and reacts with ZrB_2 to form Zr and BN in Ar atmosphere according to reaction (2) and (3). The newly formed Zr can react with SiC to form ZrC, Si and SiZr according to reaction (4) and (5).

$$2ZrN = 2Zr + N_2 \quad (2)$$

$$N_2 + ZrB_2 = Zr + 2BN \quad (3)$$

$$Zr + SiC = ZrC + Si \quad (4)$$

$$Zr + Si = SiZr \quad (5)$$

Above 2000 °C, as shown in Fig. 2, both ZrN and BN were not stable and decomposed according to reaction (2) and (6). As a result, the predicted amount of ZrB_2, ZrC and SiZr will be increased, according to reaction (7), (4) and (5).

$$2BN = 2B + N_2 \quad (6)$$

$$Zr + 2B = ZrB_2 \quad (7)$$

The calculated equilibrium composition of 2000 °C is $5.23ZrB_2 + 2.46ZrN + 1.05SiC + 1.95ZrC + 1.57Si + 1.54BN + 0.34SiZr$. The formation of BN and dissolution of carbon into ZrN at 2000 °C shown in XRD results is in accordance with the thermodynamic calculations. The ZrN and ZrC formed a carbonitride phase of Zr_2CN. The absence of Si and SiZr phases can be attributed to their reactions with oxide impurities, by which SiO gas and ZrO_2 were removed and formed during the sintering. The presence of BN, which owns a low density of 2.1 g/cm^3, is considered to be the main reason that the real density of the obtained composites decreased. The adjusted value of the theoretical density is 5.37 g/cm^3 based on the composition of $5.23ZrB_2 + 2.46Zr_2CN + 1.05SiC + 1.54BN$. As a result, the sample that sintered at 2000 °C has a relative density of 99.1%, indicating the sample was fully densified.

3.2. Microstructure

SEM observation of polished surfaces (Fig. 3(a) and (b)) shows that fine microstructure with uniform phase distribution of the ZrB_2–SiC–ZrN composite was received after reactive sintered at 2000 °C for 1 h under a pressure of 20 MPa. No obvious closed pores could be found in both polished and fracture surfaces of the sample. Although a sintering temperature as high as 2000 °C was applied, the grain growth of ZrB_2 and Zr_2CN was not significant. The gray phase of ZrB_2 owns a grain size range of 1–4 μm, with an average of 1.9 μm. The Zr_2CN phase of white color owns a similar grain size of ~1.5 μm. Several ZrB_2 particles with platelet shape can be seen in Fig. 3(b). The increase of ZrB_2 (001) peaks from 1800 °C to 2000 °C shown in Fig. 1 also indicate the anisotropic grain growth of ZrB_2 during hot pressing. This XRD result is very similar to the RHPed ZrB_2–$MoSi_2$ composites reported in our previous work in which the elongated ZrB_2 grains aligned vertical to the *c*-axis direction during the hot pressing [23]. The grain growth of ZrB_2 could be enhanced by the liquid phase formed by the solid solution of transition metal silicides via dissolution-precipitation process.

As seen from the SEM images of fracture surfaces shown in Fig. 3(c), the graphitic hexagonal BN phase formed in the composite is in a flake shape, the thickness of the BN flake is about 0.1–0.2 μm and its diameter is less than 2 μm. The EDS of the two kinds of dark black phases in Fig. 3(a) and (b) are shown in Fig. 3(d). The quasi-spherical shape grains with grain size of ~1 μm were defined as cubic *β*-SiC phase, while the small amount of needle-like phase which located at the grain boundaries was related to *h*-BN phase.

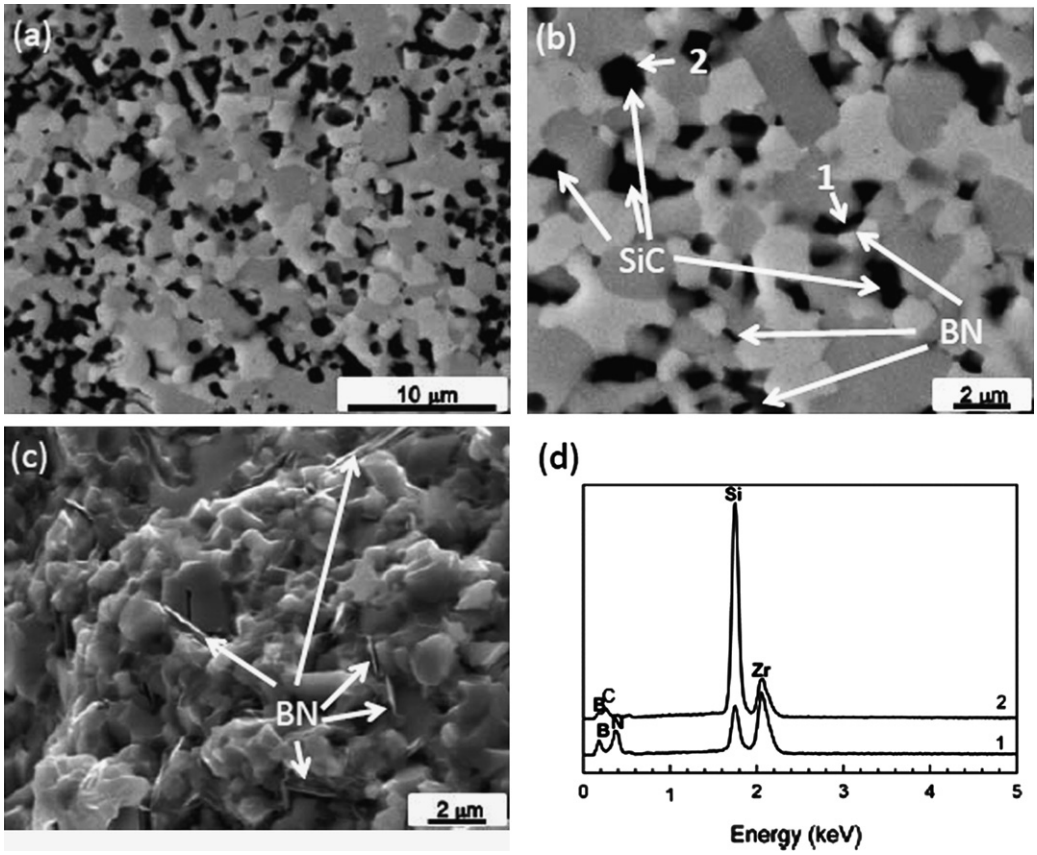

Fig. 3. SEM images of ZrB_2–SiC–ZrN composite reactive hot pressed at 2000 °C: (a), (b) polished surface; (c) fracture surface, (d) EDS of phase 1 and 2 in (b).

Table 2
Mechanical properties of ZrB_2–SiC–ZrN composite after reactive hot pressing at 2000 °C.

	Hardness (GPa)	Flexure strength (MPa)	Fracture toughness (MPa $m^{1/2}$)	Young's modulus (GPa)	Reference
RHP ZrB_2–SiC–ZrN	11 ± 0.7	536.4 ± 34	5.9 ± 0.5	266 ± 13	This work
RHP ZrB_2–SiC	21.0	506 ± 43	4.0	–	[19]
RHP ZrB_2–SiC	27 ± 2.2	800 ± 115	2.12 ± 0.06	510	[20]
SPS (Zr,Ti)B_2–(Zr,Ti)N	16.7-19.2	–	2.42–4.76	359–474	[18]

3.3. Mechanical properties

Mechanical properties of the ZrB_2–SiC–ZrN composite that synthesized through RHP at 2000 °C are listed in Table 2. Properties of related composites from literatures are also shown for comparison. Because of layered structure bonded by weak van der Waals force which enables the layers to slide easily against each other, BN owns very low hardness and Young's modulus. Hardness (11 ± 0.7 GPa) and Young's modulus (266 ± 13 GPa) of the as-received composite that contains *in situ* formed *h*-BN phase is much lower than the other reactive sintered composites that are free of *h*-BN. However, the present reactive hot pressed ZrB_2–SiC–ZrN composite shows much higher fracture toughness (5.9 ± 0.5 MPa $m^{1/2}$) and the same level of bending strength (536.4 ± 34 MPa) as the compared ones. Fig. 4 shows crack propagation of the received ZrB_2–SiC–ZrN composite after reactive hot pressing at 2000 °C. Because of the formed weak interfaces by *h*-BN phase, fracture occurred in inter-granular mode. The fracture toughness could be enhanced by crack deflection and bridging. Besides, the *in situ* formed fine *h*-BN flakes at the grain boundaries, which greatly inhibited the grain grows of ZrB_2 and Zr(C, N) during the sintering progress, played an important role on maintaining the flexure strength of the reactive hot pressed ZrB_2–SiC–ZrN composite.

4. Conclusions

A ZrB_2–SiC–ZrN composite was prepared via reactive hot pressing of a mixture of Zr, Si_3N_4, and B_4C powders at 2000 °C, under 20 MPa pressure and in Ar atmosphere. The *in situ* formation of *h*-BN phase decreased the real density of the received composite, and increased the sintering temperature. The *h*-BN flakes distributed at the grain boundary

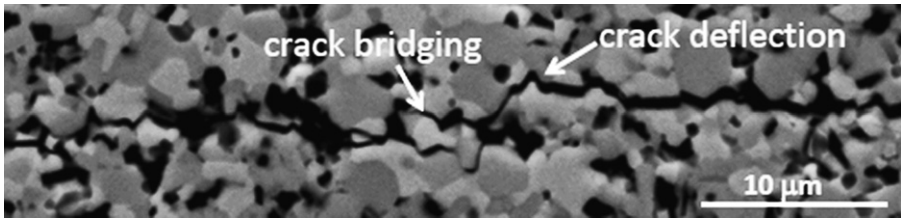

Fig. 4. Crack propagation on the polished surface of ZrB_2–SiC–ZrN composite reactive hot pressed at 2000 °C.

effectively inhibited the grains size of ZrB_2 and Zr(C, N) during the sintering. Due to the homogeneous distribution of *h*-BN phase, the received composite has a low Vickers hardness of ~11 GPa, good flexural strength of 536.4 MPa, high fracture toughness of ~5.9 MPa $m^{1/2}$, and low elastic modulus of ~266 GPa.

Acknowledgments

Financial supports from the National Natural Science Foundation of China (Nos. 50632070 and 91026008) and the Bilateral Project of NSFC-JSPS (No. 51111140017) are gratefully acknowledged.

References

[1] K. Upadhya, J.M. Yang, W.P. Hoffman, Materials for ultrahigh temperature structural applications, American Ceramic Society Bulletin 76 (12) (1997) 51–56.
[2] M.M. Opeka, I.G. Talmy, J.A. Zaykoski, Oxidation-based materials selection for 2000 degrees C plus hypersonic aero surfaces: Theoretical considerations and historical experience, Journal of Materials Science 39 (19) (2004) 5887–5904.
[3] W.G. Fahrenholtz, G.E. Hilmas, I.G. Talmy, J.A. Zaykoski, Refractory diborides of zirconium and hafnium, Journal of the American Ceramic Society 90 (5) (2007) 1347–1364.
[4] J. Zou, G.J. Zhang, C.F. Hu, T. Nishimura, Y. Sakka, H. Tanaka, J. Vleugels, O. Biest, High-temperature bending strength, internal friction and stiffness of ZrB_2-20 vol% SiC ceramics, Journal of the European Ceramic Society 32 (10) (2012) 2519–2527.
[5] D. Sciti, S. Guicciardi, A. Bellosi, G. Pezzotti, Properties of a pressureless-sintered ZrB_2–$MoSi_2$ ceramic composite, Journal of the American Ceramic Society 89 (7) (2006) 2320–2322.
[6] S.Q. Guo, Y. Kagawa, T. Nishimura, H. Tanaka, Pressureless sintering and physical properties of ZrB_2-based composites with $ZrSi_2$ additive, Scripta Materialia 58 (7) (2008) 579–582.
[7] C.F. Hu, Y. Sakka, B. Jang, H. Tanaka, T. Nishimura, S.Q. Guo, S. Grasso, Microstructure and properties of ZrB_2–SiC and HfB_2–SiC composites fabricated by spark plasma sintering (SPS) using $TaSi_2$ as sintering aid, Journal of the Ceramic Society of Japan 118 (1383) (2010) 997–1001.
[8] C.F. Hu, Y. Sakka, H. Tanaka, T. Nishimura, S.Q. Guo, S. Grasso, Microstructure and properties of ZrB_2–SiC composites prepared by spark plasma sintering using $TaSi_2$ as sintering additive, Journal of the European Ceramic Society 30 (12) (2010) 2625–2631.
[9] C.F. Hu, Y. Sakka, H. Tanaka, J.H. Gao, H. Tanaka, S. Grasso, Microstructure characterization of ZrB_2–SiC composite fabricated by spark plasma sintering with $TaSi_2$ additive, Journal of the European Ceramic Society 32 (7) (2012) 1441–1446.
[10] S.C. Zhang, G.E. Hilmas, W.G. Fahrenholtz, Pressureless densification of zirconium diboride with boron carbide additions, Journal of the American Ceramic Society 89 (5) (2006) 1544–1550.
[11] S. Zhu, W.G. Fahrenholtz, G.E. Hilmas, S.C. Zhang, Pressureless sintering of zirconium diboride using boron carbide and carbon additions, Journal of the American Ceramic Society 90 (11) (2007) 3660–3663.
[12] A.L. Chamberlain, W.G. Fahrenholtz, G.E. Hilmas, D.T. Ellerby, High-strength zirconium diboride-based ceramics, Journal of the American Ceramic Society 87 (6) (2004) 1170–1172.
[13] J. Zou, G.J. Zhang, C.F. Hu, T. Nishimura, Y. Sakka, J. Vleugels, O. Biest, Strong ZrB_2–SiC–WC Ceramics at 1600 degrees C, Journal of the American Ceramic Society 95 (3) (2012) 874–878.
[14] M.J. Thompson, W.G. Fahrenholtz, G.E. Hilmas, Elevated temperature thermal properties of ZrB_2 with carbon additions, Journal of the American Ceramic Society 95 (3) (2012) 1077–1085.
[15] F. Monteverde, A. Bellosi, Beneficial effects of AlN as sintering aid on microstructure and mechanical properties of hot-pressed ZrB_2, Advanced Engineering Materials 5 (7) (2003) 508–512.
[16] F. Monteverde, A. Bellosi, Effect of the addition of silicon nitride on sintering behaviour and microstructure of zirconium diboride, Scripta Materialia 46 (3) (2002) 223–228.
[17] F. Monteverde, A. Bellosi, Efficacy of HfN as sintering aid in the manufacture of ultrahigh-temperature metal diborides-matrix ceramics, Journal of Materials Research 19 (12) (2004) 3576–3585.
[18] C.F. Hu, Y. Sakka, H. Tanaka, T. Nishimura, S. Grasso, Synthesis, microstructure and mechanical properties of (Zr,Ti)B_2–(Zr,Ti)N composites prepared by spark plasma sintering, Journal of Alloys and Compounds 494 (1–2) (2010) 266–270.
[19] G.J. Zhang, Z.Y. Deng, N. Kondo, J.F. Yang, T. Ohji, Reactive hot pressing of ZrB_2–SiC composites, Journal of the American Ceramic Society 83 (9) (2000) 2330–2332.
[20] A.L. Chamberlain, W.G. Fahrenholtz, G.E. Hilmas, Low-temperature densification of zirconium diboride ceramics by reactive hot pressing, Journal of the American Ceramic Society 89 (12) (2006) 3638–3645.
[21] W.W. Wu, G.J. Zhang, Y.M. Kan, P.L. Wang, Reactive hot pressing of ZrB_2–SiC–ZrC ultra high-temperature ceramics at 1800 degrees C, Journal of the American Ceramic Society - 89 (9) (2006) 2967–2969.
[22] W.W. Wu, G.J. Zhang, Y.M. Kan, P.L. Wang, Reactive hot pressing of ZrB_2–SiC–ZrC composites at 1600 degrees C, Journal of the American Ceramic Society - 91 (8) (2008) 2501–2508.
[23] W.W. Wu, Z. Wang, G.J. Zhang, Y.M. Kan, P.L. Wang, ZrB_2–$MoSi_2$ composites toughened by elongated ZrB_2 grains via reactive hot pressing, Scripta Materialia 61 (3) (2009) 316–319.
[24] H.L. Zhao, J.L. Wang, Z.M. Zhu, J. Wang, W. Pan, Mechanical properties and microstructure of *in situ* synthesized ZrB_2–ZrN_{1-x} composites, Journal of Materials Science 41 (6) (2006) 1769–1773.
[25] M.W. Chase Jr., in: NIST-JANAF Thermochemical Tables, 4th edition, American Institute of Physics, Woodbury, NY, 1998.
[26] HSC chemistry for Windows 6.1, Outokumpu Research Oy, Pori, Finland.